doi:10.1246/cl.2012.119
Published on the web December 30, 2011

New Organic Ferroelectrics: Cocrystal of 5,5′-Dimethyl-2,2′-bipyridine and Bromanilic Acid

Yasuhisa Yamamura,[1] Erika Saito,[1] Hideki Saitoh,[2] Norie Hoshino,[1] and Kazuya Saito*[1]
[1]*Department of Chemistry, Faculty of Pure and Applied Sciences, University of Tsukuba, Tsukuba, Ibaraki 305-8571*
[2]*Graduate School of Science and Engineering, Saitama University, Saitama 338-8570*

(Received October 7, 2011; CL-110823; E-mail: kazuya@chem.tsukuba.ac.jp)

Cocrystal 55DMBP–H_2ba was synthesized and characterized. The crystal structure is isostructural to cocrystal 55DMBP–H_2ia with iodanilic acid. The heat capacity, dielectric permittivity, and polarization–electric field hysteresis showed that the 55DMBP–H_2ba undergoes a paraelectric–ferroelectic phase transition at 253 K on cooling. The transition mechanism is discussed through the analysis of isotropic temperature factors of atoms.

Recently, organic ferroelectrics having a hydrogen bond (H bond), e.g., phenazine–chrolanilic acid[1] (Phz–H_2ca), have been paid increasing attention.[2,3] In those compounds, dielectric properties depend on a combination of H-bond donor and acceptor.[2] A representative series is cocrystals between 5,5′-dimethyl-2,2′-bipyridine (55DMBP) and H_2xa: 55DMBP–H_2ca is antiferroelectric[4] whereas 55DMBP–H_2ia (iodanilic acid) ferroelectic.[5] Since both ferroelectricity and antiferroelectricity are found, the series is very important for understanding the mechanism that determines the dielectric nature of such organic complexes. However, there has been no report on 55DMBP–H_2ba (bromanilic acid) so far. In this letter, we report its synthesis, structure, and properties.

Single crystals of 55DMBP–H_2ba were grown by diffusion using dehydrated acetone (Wako, >99.5%) as a solvent. Commercial 55DMBP (Aldrich, 98%) and H_2ba (TCI, >98%) were purified by fractional sublimation in vacuum before dissolving them in dehydrated acetone. The growth took about 2 months. The yield was very low (1–5%) even in successful cases. Due to the difficulty in crystal growth, only a limited number of single crystals were available for measurements of physical properties. This prevented the authors from performing precise characterization at the highest level.

Structure analyses were performed using a SMART APEX diffractometer (Bruker AXS KK). Data collections were performed at room temperature (295 K) and 200 K. Unit-cell refinement and data reduction were carried out using SAINT.[6] SHELXTL[7] was used to solve and refine structures. The experimental conditions and crystallographic parameters are tabulated in Tables S1–S3.[17]

Heat capacity (C_p) of a single crystal (7.044 mg) was measured from 300 to 100 K using a commercial relaxation calorimeter (PPMS, Quantum Design). The crystal was adhered to the sample holder with Apiezon-N grease.

Polarization (P)–electric field (E) hysteresis measurement was carried out using a laboratory-made cryostat by the so-called Sawyer–Tower circuit method.[8] Silver paste as electrode was spread on two opposite faces of a single crystal ($3.4 \times 2.3 \times 0.54\,mm^3$), as shown in the inset of Figure 3. The crystal faces of the sample were identified using the X-ray diffractometer by the Laue method. The applied AC source was the power line (50 Hz, 100 V). Dielectric permittivity was measured at 1 kHz using the same sample, electrode and cryostat as those used for the P–E hysteresis measurement.

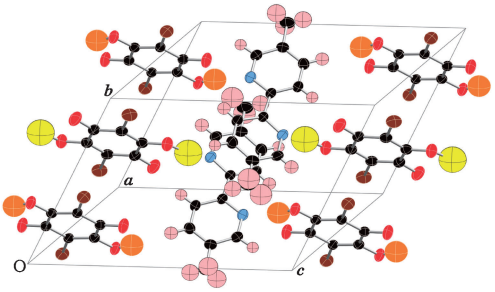

Figure 1. Crystal structure of 55DMBP–H_2ba at room temperature. Black, carbon atom; blue, nitrogen atom; red, oxygen atom; brown, bromine atom; pink, hydrogen atom of 55DMBP; yellow and orange, H(13) and H(14), respectively.

Crystal structure of 55DMBP–H_2ba at room temperature is triclinic (space group $P\bar{1}$) as shown in Figure 1. The details are listed in Tables S1 and S2.[17] The structure is isostructural to that of 55DMBP–H_2ia at room temperature[5] but is different from that of 55DMBP–H_2ca.[4,9] The unit cell is nearly the same size as that of 55DMBP–H_2ia. The molecules of 55DMBP and H_2ba are alternately connected through H bonds and form one-dimensional chains. There are two crystallographically independent H bonds; O(2)–H(13)···N(1) (O···N 2.70 Å) and O(4)–H(14)···N(2) (O···N 2.59 Å). In the former, H(13) is located nearly at the middle between O(2) and N(1). On the other hand, H(14) is close to O(4) of the bromanilic acid molecule (0.94 Å in O(4)–H(14) and 1.75 Å in H(14)–N(2)). 55DMBP molecule has a twisted structure around the C–C bond between two pyridine groups, as in 55DMBP–H_2ia. The dihedral angle in 55DMBP–H_2ba (14°) is smaller than those in 55DMBP–H_2ia (19°).[5] The resemblance in crystal structure implies the emergence of ferroelectricity in 55DMBP–H_2ba at low temperatures.

The C_p of 55DMBP–H_2ba is shown in Figure 2. An anomaly was observed around 253 K. Its shape is just like an anomaly of the second-order phase transition given by the molecular field approximation. The temperature of phase transition (T_{trs}) was determined to be 253 K from the maximum of anomalous heat capacity ΔC_p. It is lower than that of 55DMBP–H_2ia (270 K). The height of the anomaly (ΔC_p) at T_{trs} is comparable to R (R, gas constant), implying that the entropy of transition ($\Delta_{trs}S$) is comparable to $R \ln 2$ expected for the Ising model. However, the present work cannot give us the enthalpy and entropy of transition, because there is a small discontinuity of the C_p around 190 K. The discontinuity is probably due to cracking of the sample. Indeed, the sample was broken after the measurement. The existence of the first-order phase transition

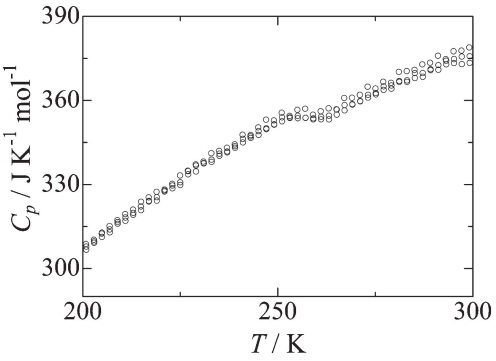

Figure 2. Heat capacity of 55DMBP–H_2ba.

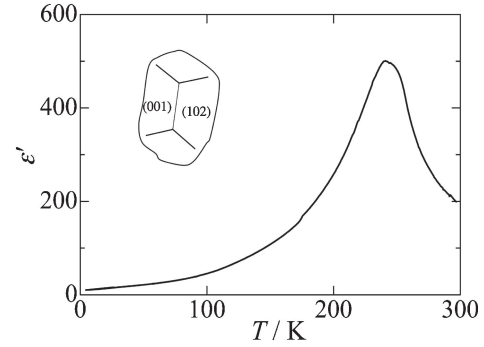

Figure 3. Dielectric permittivity of 55DMBP–H_2ba along the easy axis of polarization. The inset shows the single crystal used for dielectric and *P*–*E* hysteresis measurements. Both (102) and (001) faces were simultaneously used as an electrode.

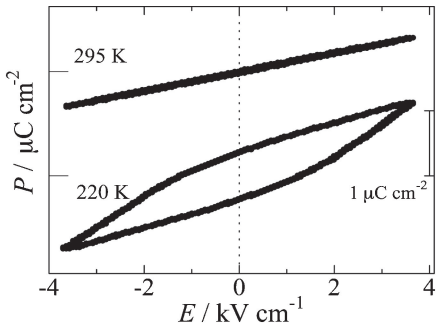

Figure 4. *P*–*E* hysteresis of 55DMBP–H_2ba at 295 and 220 K.

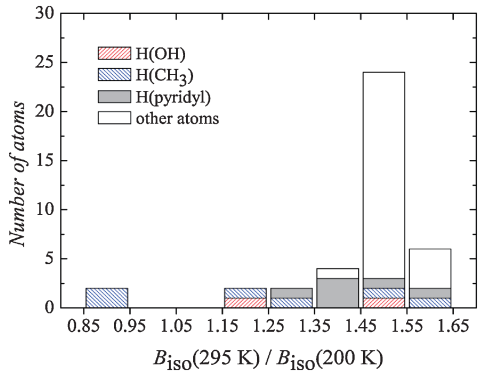

Figure 5. Distribution of the ratio of isotropic temperature factors $B_{iso}(295\,K)/B_{iso}(200\,K)$ of atoms in 55DMBP–H_2ba.

below the second-order phase transition has been observed in Phz–H_2ca and its analogs.[10,11] Although a similar situation may be imagined, this issue is left for the future.

Experimental dielectric permittivity is plotted in Figure 3. There is a maximum around 250 K. Since the temperature agrees with T_{trs} in C_p, the maximum is attributed to the phase transition. The phase transition accompanies the change in the dielectric property. The *P*–*E* hysteresis measurements were carried out at 295 and 220 K (Figure 4). Although the hysteresis is not observed at 295 K, the hysteresis loop is clearly opened at 220 K. This means that 55DMBP–H_2ba has spontaneous polarization below T_{trs}. The hysteresis loop indicates that the low-temperature phase is ferroelectric (FE) without the centrosymmetry present in the paraelectric (PE) room-temperature phase. Because of the limited availability of single crystals, the shape of the sample was not modified (cut and/or shaved). This prevents the precise determination of the polar axis. However, in the present *P*–*E* hysteresis measurements, the direction of the electric field was roughly perpendicular to (102) and (001) planes of PE phase. This suggests that the axis of polarization is along the direction of the one-dimensional chain of ···–H_2ba–55DMBP–H_2ba–··· connected by H bonds. Therefore, the ferroelectricity probably originates in the H bonds. As in the case of calorimetry, the cracking below 200 K was observed in the *P*–*E* hysteresis measurements, resulting in the failure in observing saturated curve.

Although the appearance of spontaneous polarization is definite evidence of the absence of centrosymmetry in FE phase, the diffraction data collected at 200 K could be analyzed assuming either of space groups $P\bar{1}$ or $P1$ with essentially the same lattice setting as PE phase at room temperature. No definite conclusion was reached concerning the space group of FE phase from these structure analyses. This indicates that the space group of FE phase is $P1$ with only weak violation of centrosymmetry. Indeed, the atomic coordinates are very similar between PE and FE phases. The details of analysis and atomic coordinates are listed in Tables S1, S3, and S4.[17]

Some insights on the transition mechanism can be deduced from the atomic temperature factors ($B_{iso}(T)$) estimated in structure analyses[12] assuming $P\bar{1}$ for both PE and FE phases. Within the harmonic oscillator approximation, $B_{iso}(T)$ is proportional to temperature. It is, therefore, expected that the ratio $B_{iso}(295\,K)/B_{iso}(200\,K)$ is close to 1.475 ($\approx 295/200$) unless atoms are directly involved in the transition mechanism. The ratios were calculated for all atoms (40 atoms) and summarized as a histogram in Figure 5. The $B_{iso}(295\,K)/B_{iso}(200\,K)$ of Br, C, N, and O atoms are close to 1.475 and distributed in a narrow region between 1.43 and 1.58. This result indicates the normal temperature dependence of their B_{iso}. The H atoms of pyridyl group are also normal, because their $B_{iso}(295\,K)/B_{iso}(200\,K)$ distributes in the region from 1.43 to 1.64. In contrast, the $B_{iso}(295\,K)/B_{iso}(200\,K)$ of H atoms in the methyl group are distributed in a very wide range from 0.88 to 1.60. This abnormal distribution is attributed to librational and/or rotational motion of the methyl groups. It is noted that the methyl groups can hardly contribute to polarization because of their threefold symmetry.[13]

Of special interest is $B_{iso}(295\,K)/B_{iso}(200\,K)$ for the H atoms in H bonds in relation to the ferroelectricity as suggested from the *P*–*E* hysteresis measurements. The ratio differs significantly for these two H atoms: 1.5 for H(13) and 1.2 for H(14). Since the ratio is close to 1.475, the pseudo-centrosymmetry of H(13) should remain even in FE phase having $P1$ symmetry. On the other hand, the ratio of H(14) atom significantly different from 1.475 clearly demonstrates that H(14) atom is involved in the appearance of ferroelectricity.

The small $B_{iso}(295\,K)/B_{iso}(200\,K)$ of H(14) requires an anomalously large $B_{iso}(200\,K)$ and/or an anomalously small $B_{iso}(295\,K)$. Although the possibility of the latter due to the significant change in the potential curve that H(14) atom sees cannot be ruled out, the former seems more plausible, while considering the fact that the temperatures (295 and 200 K) are far enough to neglect effects of the critical fluctuation. The transition mechanism that brings ferroelectricity is often classified into one of displacive or order–disorder types, though an intermediate mechanism is also possible.[14–16] Assuming the order–disorder type mechanism for the present case, the PE phase is the disordered phase concerning the position of H(14) atom while the FE phase the ordered phase. Since the structure analyses assume the centrosymmetry for both PE and FE phases, the resulting temperature factor consists of components arising from positional disorder and thermal vibration. The component arising from the disorder is the same for both phases because the centrosymmetry is assumed even for FE phase. Assuming the component from the positional disorder is dominant, the small $B_{iso}(295\,K)/B_{iso}(200\,K)$ is expected. The weak temperature dependence is attributed to the component from the thermal vibration. This order–disorder mechanism is consistent with the C_p result because the anticipated $\Delta_{trs}S\,(= R\ln 2)$ from the ΔC_p is fully compatible with the disorder of only one H atom in two atoms of H_2ba.

The crystal structure of the present cocrystal 55DMBP–H_2ba, which is ferroelectric at low temperatures, is essentially the same as that of ferroelectric 55DMBP–H_2ia and distinct from that of antiferroelectric 55DMBP–H_2ca. This suggests the dielectric property is primarily governed by their crystal structures. To design rationally molecular ferroelectrics, further advancement in crystal engineering is necessary, accordingly. Concerning the difficulty in successful synthesis of the present cocrystal, however, the following can be imagined: the competition between tendencies toward (at least two) aggregation modes that bring either ferroelectric or antiferroelectric property prevents successful growth of the cocrystal. If this is the case, the detailed study of amorphous matter left in growth vessels would offer valuable information in context of the crystal engineering.

In summary, we have shown the crystal structure, phase transition, and ferroelectricity of 55DMBP–H_2ba. The ferroelectricity plausibly originates in the positional ordering of H atoms in the one-dimensional H-bond chains. Such H-bond chains often exhibit interesting dynamics of protons, which is, e.g., seen in Phz–H_2ca.[11] However, the study on the proton dynamics in 55DMBP–H_2ba is beyond the scope of the present work.

References and Notes

1 S. Horiuchi, F. Ishii, R. Kumai, Y. Okimoto, H. Tachibana, N. Nagaosa, Y. Tokura, *Nat. Mater.* **2005**, *4*, 163.
2 S. Horiuchi, R. Kumai, Y. Tokura, *Chem. Commun.* **2007**, 2321.
3 S. Horiuchi, Y. Tokura, *Nat. Mater.* **2008**, *7*, 357.
4 R. Kumai, S. Horiuchi, Y. Okimoto, Y. Tokura, *J. Chem. Phys.* **2006**, *125*, 084715.
5 S. Horiuchi, R. Kumai, Y. Tokura, *Angew. Chem., Int. Ed.* **2007**, *46*, 3497.
6 *SAINT (Ver. 6.45)*, Bruker AXS, Madison, WI, **2003**.
7 *SHELXTL (Ver. 6.14)*, Bruker AXS, Madison, WI, **2003**.
8 C. B. Sawyer, C. H. Tower, *Phys. Rev.* **1930**, *35*, 269.
9 G. Bator, W. Sawka-Dobrowolska, L. Sobczyk, E. Grech, J. Nowicka-Scheibe, A. Pawlukojć, J. Wuttke, J. Baran, M. Owczarek, *J. Chem. Phys.* **2011**, *135*, 044509.
10 K. Saito, M. Amano, Y. Yamamura, T. Tojo, T. Atake, *J. Phys. Soc. Jpn.* **2006**, *75*, 033601.
11 M. Amano, Y. Yamamura, M. Sumita, S. Yasuzuka, H. Kawaji, T. Atake, K. Saito, *J. Chem. Phys.* **2009**, *130*, 034503.
12 H. Saitoh, K. Saito, Y. Yamamura, H. Matsuyama, K. Kikuchi, I. Ikemoto, *Solid State Commun.* **1994**, *91*, 89.
13 K. Saito, Y. Yamamura, N. Kikuchi, A. Nakao, S. Yasuzuka, Y. Akishige, Y. Murakami, *CrystEngComm* **2011**, *13*, 2693.
14 Y. Onodera, *Prog. Theor. Phys.* **1970**, *44*, 1477.
15 K. Saito, Y. Yamamura, H. Saitoh, H. Matsuyama, K. Kikuchi, I. Ikemoto, *Solid State Commun.* **1993**, *87*, 903.
16 K. Saito, Y. Yamamura, H. Saitoh, H. Matsuyama, K. Kikuchi, I. Ikemoto, *Solid State Commun.* **1994**, *92*, 495.
17 Supporting Information is available electronically on the CSJ-Journal Web site, http://www.csj.jp/journals/chem-lett/index.html.

